

A combined approach for the development of efficient and safe nanoantimicrobials: the case of nanosilver-modified polyurethane foams

Rosaria Anna Picca^{†}, Federica Paladini[§], Maria Chiara Sportelli[†], Mauro Pollini[§], Lorena
Carla Giannossa[¶], Cinzia Di Franco[‡], Angelica Panico[§], Annarosa Mangone[†], Antonio
Valentini[‡], Nicola Cioffi^{*†}*

[†]Dipartimento di Chimica, Università degli Studi di Bari Aldo Moro, Via Orabona 4, 70126 Bari (Italy); [§]Dipartimento di Ingegneria dell'Innovazione, Università del Salento, Via per Monteroni, 73100 Lecce (Italy); [‡]CNR-IFN - Dipartimento Interateneo di Fisica, Università degli Studi di Bari Aldo Moro, Via Amendola 173, 70126 Bari (Italy); [‡]Dipartimento Interateneo di Fisica, Università degli Studi di Bari Aldo Moro, Via Amendola 173, 70126 Bari (Italy); [¶]Author present address: Dipartimento di Economia, Management e Diritto dell'Impresa, Università degli Studi di Bari Aldo Moro, Largo Abbazia Santa Scolastica 53, 70124 Bari (Italy).

KEYWORDS. nanomaterial; antimicrobial; nanosafety; electron microscopy; XPS; ICP-MS; nanoparticle release.

ABSTRACT. Silver nanophases are routinely used as bioactive additives in commercial products. Besides their antimicrobial activity, nanosafety issues regarding the application of (silver-based) nanoantimicrobials should be considered, as well. In this study, we modified polyurethane foams, typically employed in air filtration and stuffing, by photo-deposited silver nanoparticles for preparing hybrid materials (Ag-PU) with antibacterial properties. The composite materials were characterized in terms of morphology, surface chemical composition, ionic release in contact media, bioactivity, as well as whole nanoparticle release. Cytocompatibility was also assessed on 3T3 mouse fibroblasts. The proposed systematic approach allows for defining suitable composite final properties, in terms of bioactivity and safety, by proper tuning the deposition parameters.

INTRODUCTION

Silver is becoming more and more abundant in commercial products, both as saline additive and in the form of nanophases, for the production of a wide variety of products with antimicrobial properties ¹⁻⁴. Among all the organic and inorganic materials modified with (nano-) silver, polyurethane and its derivatives are quite common ⁵⁻⁷. Polyurethanes (PUs) comprise an important polymer category used in industry as coatings, adhesives, foams, rubbers and composites ^{8,9}. Their application areas include construction industry, automotive, packaging, transportation, electronics, textiles, tapes, papers and footwear ^{10,11}. In particular, due to the good biocompatibility and the tailorable mechanical properties, PU-based materials have been also widely employed for biomedical uses and for the manufacturing of implant materials such as stents, catheters, pacemaker leads, heart valves and as scaffolds for cardiovascular engineering ¹²⁻¹⁶. Indeed, due to their hemocompatibility, PUs are the most commonly used materials in the production of blood-

contacting devices, such as artificial veins, arteries and grafts ^{17,18}, which are commercially available in Asia and Europe since several years, and have been approved for daily use in the US in December 2000 ¹⁹. Thermoplastic polyurethanes (TPUs) have been proposed as drug delivery matrixes as well, with specific formulations adapted to drug characteristics ¹³. TPUs can be synthesized from a wide variety of precursors, using a plethora of hard and soft segments, for various biological applications ¹³. Many research groups explored new compositions and methods to produce novel PUs, in order to improve their biocompatibility and biomedical properties ¹⁷. Anyhow, as a biocompatible polymer, PU typically provides a good substrate for microbial adhesion, thus promoting potential infections. Hence, research concerning the development of antimicrobial PU-based materials represents a great challenge for both industry and academia ^{20,21}. Silver nanoparticles (AgNPs) have been widely used as antimicrobial and antifungal agents ²² to meet this need: the addition of AgNPs enables producers to publicize their products as more hygienic, capable of preventing infections from drug-resistant bacteria, claiming the same antimicrobial AgNP technology used in nosocomial frameworks ²³. Nowadays, the issue of multi-drug resistant bacteria is becoming a leading research topic, because the widespread use of broad-spectrum antibiotics has produced resistance in many human pathogens ²⁴. Although AgNP mechanisms of action have not been fully elucidated yet, silver has demonstrated effectiveness against a wide range of resistant microorganisms ²⁴⁻²⁷. In this scenario, the application of AgNPs in both air and water filtration systems represents a great potential to reduce the risk of bioaerosol-related diseases ^{28,29}. It is worth noting that using AgNP-containing products may lead to (nano-) particle release, which raises concern towards both environmental pollution and human toxicity. Currently, there is no single analytical method or protocol able to answer the requirement of assessing NP release, but a variety of existing methods, used in combination, offered us the

possibility of addressing this target. Since literature dealing with particle release is still limited, it is somehow difficult to develop protocols aiming at assessing nanotoxicological issues³⁰. Here we ~~propose~~ describe a modification protocol for commercial PU foams (used as filtering material in air conditioning and as padding) with nanosilver, which is easily implementable on industrial processes. Detailed morphological and chemical characterization of modified PU materials is herein reported, along with tests on bioactivity and cytocompatibility; assessment of silver release (both in particulate and ionic form) was here conducted in real-life conditions, combining for the first time results arising from transmission and scanning electron microscopies (TEM, SEM), inductively coupled plasma mass spectrometry (ICP-MS), and UV-Vis measurements. This work will contribute to address the urgent need to evaluate NP-modified product safety, using methodologies that could be easily transferred with acceptable precision, accuracy and reproducibility, after proper validation, among control laboratories.

EXPERIMENTAL

Preparation of Ag-modified PUs

Industrial PU foams were kindly provided by ME.RES. Srl (Avellino, Italy). Square samples (10 cm x 10 cm) were modified with AgNPs by adopting a patented protocol³¹ based on a photo-assisted process³². Firstly, a silver nitrate (>99%, Alfa Aesar, Italy) solution was prepared in water and methanol (99.9%, Sigma Aldrich, Italy), which acted as both solvent and reducing agent. Then, the solution was spray-deposited (100 g/m²) onto sample surfaces and wet substrates were finally exposed to an ultraviolet source (Jelosil HG 1000, $\lambda = 365$ nm, working distance = 50 cm) for 15 minutes. This step aimed at promoting silver precursor (Ag⁺) photo-reduction to Ag⁰. A silver precursor solution with a nominal loading of 4%_{w/w}, was used, unless otherwise stated.

Surface chemical characterization by XPS

Samples surface chemical characterization was performed using a Thermo-VG Theta Probe X-ray photoelectron spectrometer equipped with a micro-spot monochromatized AlK α source, using a 300- μ m X-ray beam, in constant analyzer energy mode (CAE). Samples were mounted onto the sample holder using a double-sided conductive copper tape; charge compensation was performed using a flood gun operating at -1 eV. Spectra processing was performed by commercial Thermo Advantage[®] software (v. 5.937, 2014). XPS surface elemental compositions were obtained after Shirley background removal, and all values reported were averaged out of three different replicates.

Morphological characterization by SEM

Ag-modified PUs morphological characterization was performed by a field emission scanning electron microscope (FE-SEM), model Sigma Zeiss (Jena, Germany). In order to observe AgNP in-depth distribution within the PU foam, 2-mm-thick cross-sections were obtained through freeze fracturing. Cross sections were coated by a few nm palladium layer by an electron beam evaporator to avoid charging; then, they were examined at a 10 kV acceleration voltage, 30- μ m aperture, in top-view. To map the actual surface of the samples, the in-lens detector was used, revealing the secondary electrons.

Silver release from modified PUs

Silver ion (Ag⁺) release was quantified by inductively coupled plasma mass spectrometry (ICP-MS) on cubic, 1-cm³ PU samples (\sim 40 mg/cm³); both pristine and Ag-modified samples were tested. In order to evaluate the maximum amount of Ag releasable from the modified materials, they were immersed for 24 h in 2%_{w/w} HNO₃ (Protocol **A**). Kinetics of ion release (Protocol **B**) were instead evaluated immersing samples in a phosphate buffered saline (PBS) solution,

mimicking normal physiological conditions. PBS solution was prepared using high purity salts (TraceSelect®, Sigma, Italy), mixing phosphate buffer (pH = 6.8, ionic strength $I = 0.1$) with 0.85%_{w/w} NaCl, in 1:1 ratio. Samples were immersed in 6 mL of PBS solution and, at defined times, aliquots of the contact medium were sampled and analyzed by ICP-MS. All experimental data were averaged on three replicates. Silver concentration was evaluated by a NexION 300X Perkin-Elmer ICP-MS spectrometer, equipped with a collision cell, monitoring isotopes ^{107}Ag and ^{109}Ag . Operating conditions used for ICP-MS analyses are reported in Table S1. Indium was used as internal standard, with a final concentration of 25 ppb. For Protocol **A**, spectrometer calibration was performed with Ag^+ standard solutions in 2%_{w/w} HNO_3 . For Protocol **B**, Ag^+ solutions were obtained by adding known amounts of silver nitrate in 6 mL of PBS, then reaching a final volume of 50 mL with 2%_{w/w} HNO_3 . Collected samples were properly diluted with HNO_3 2%_{w/w} HNO_3 before each measurement, down to Ag^+ concentrations in the range 1-100 ppb.

Possible release of entire AgNPs in the atmosphere was evaluated, too. Direct contact with whole AgNPs (e.g. via inhalation) could be, in fact, particularly harmful for humans ³³. We used a simple protocol for AgNPs collection, where a controlled flow of pure gas was let flushing through treated PU filters. Briefly, filters were cut as circular sections with a diameter of 6 mm and then positioned, in number of 3, into a micropipette tip, mimicking a typical multi-stage air filtration system, as commonly found in centralized air conditioning (A/C) apparatuses ³⁴. Nitrogen (99.999%) was used as carrier gas, with a flow rate of 30 mL/min, controlled by an analogical flowmeter. We chose an experiment duration of 8 hours as a model exposure time to air conditioning during worktime. A flow rate of 30 mL/min was chosen considering that A/C flow rates generally range between $3 \cdot 10^{-3}$ and 10^{-4} cmf (Cubic Feet per Minute), corresponding to ≈ 3 and 80 mL/min, respectively ³⁴. A detailed description of the experimental apparatus is provided as Supporting Info

(Fig. S1). The outgoing gas flow was let bubbling in a glass tube containing 2 mL of MilliQ water (25°C, 18 MΩ), and left constant for 8 hours. At the end of this time, when the liquid volume was halved, 1 µL of the solution was sampled, deposited on 300 mesh Formvar[®]-coated copper TEM grids (Agar Scientific, UK), and dried in air. Samples were analyzed by a FEI Tecnai 12 TEM microscope, with a LaB₆ filament, operating at 120 kV. The microscope was calibrated and aligned by using factory settings and routines. Astigmatism was adjusted by means of fast Fourier transform processing. The movement of the electron beam over the grid was systematically tracked, in order to ensure complete investigation of all the grid sectors and preventing duplicate observation of the same field (and particles). For each kind of PU sample, TEM assessment of whole particle release was carried out at least on two replicated and independent experiments. The very same aqueous samples (1 mL, collected after filtration either on Ag-modified or untreated PU filters) were characterized by UV-Vis spectroscopy to investigate the plasmon peak associated to AgNPs (typically falling in the 400-450 nm wavelength range). UV-Vis spectra were acquired in the wavelength range from 300 to 600 nm on a double-beam spectrophotometer (Shimadzu, model UV-1601). Diluted (corresponding to ~10 ppb and ~100 ppb of silver) aqueous silver nanoparticles (AgNPs) colloids were also characterized by UV-Vis spectroscopy for comparison purposes. AgNPs were prepared in the presence of ammonia, to complex silver ions, and adding glucose as reducing agent, according to a previously reported procedure³⁵.

Antibacterial tests

The antibacterial activity of Ag-treated samples was evaluated on *Escherichia coli* (DH5α, 10⁶ colony forming units per mL - CFU/mL), and *Staphylococcus aureus* (SA1, 10⁶ CFU/mL) through agar diffusion tests and bacterial enumeration. *E. coli* and *S. aureus* were grown at 37°C,

respectively in Luria-Bertani (LB) broth and nutrient broth. The agar diffusion procedure consisted in incubating the samples at 37°C overnight in contact with bacteria on agar plates and, then, in evaluating the presence of an inhibition area to bacteria growth beneath and around the samples. The bacterial enumeration was performed through spectrophotometric analyses by using a spectrophotometer VWR V-1200. In triplicate, samples (1 cm³) were incubated overnight at 37°C in 3 mL of growth medium. After 24 hours of incubation, the optical density (OD) was measured at 600 nm, and the results were expressed as bacterial reduction percentage calculated in comparison with the untreated samples. The same microbiological suspensions were also re-incubated at 37°C for additional 24 hours in order to evaluate the proliferation capability of the surviving bacteria. After incubation, 1 mL of the suspensions was analyzed through spectrophotometric analysis.

Cytocompatibility tests

Cell viability was analyzed through 3-[4,5-dimethylthiazol-2-yl]-2,5-diphenyltetrazolium bromide colorimetric assay (MTT), by adopting the only Dulbecco's modified Eagle's medium (DMEM) as positive control and the cells incubated without samples as negative control. 3T3 Mouse embryonic fibroblasts were cultured in DMEM supplemented with 10% fetal bovine serum (FBS) and antibiotics (1% U/ml Streptomycin-Penicillin). Cells were plated at 1x10⁵ cells/ml in 24-well plates, and incubated in a humidified incubator with 5% CO₂ at 37°C.

Untreated and silver treated samples (1 cm³) were immersed, in triplicate, in 6 mL of phosphate buffered saline (PBS) solution and incubated at 37°C for 24 hours and, after incubation, 300 µl of extracts were added to 24-well plates with 700 µl DMEM. After 1, 3 and 5 days of cell culture, MTT solution (5 mg/mL in PBS, Sigma Aldrich) was added to reach a final concentration of

0.5mg/mL and plates were incubated at 37 °C for 2 h. After the assay, the blue formazan reaction product was dissolved by adding 1 mL of isopropanol to each well. Then, the supernatants were centrifuged at 1300 ×g for 5 min and the solubilized formazan was measured at 550 nm using a spectrophotometer (V-1200, VWR).

RESULTS AND DISCUSSION

Preparation of Ag-modified PUs

PU substrates were modified with AgNPs through the in situ photo-reduction of silver nitrate described above. Pristine and treated foams were subjected to optical and SEM microscopy examination. This aimed at ascertaining that the impregnation process did not alter PU pores morphology and/or dimension. Typical optical and SEM micrographs are reported in **Fig. 1**. A slight darkening of the PU foam after Ag treatment was appreciable (**Fig. 1a-b**): this evidence was attributed to the dark-yellow color typical of AgNPs. SEM microscopy allowed for a deeper look into foams morphology. Polymer cellulation degree (i.e. number of empty cells per surface unit) remained constant after Ag photo-deposition: comparing SEM pictures such as those in **Fig. 1c** and **Fig. 1d**, in fact, no change in cell dimensions and shape could be appreciated.

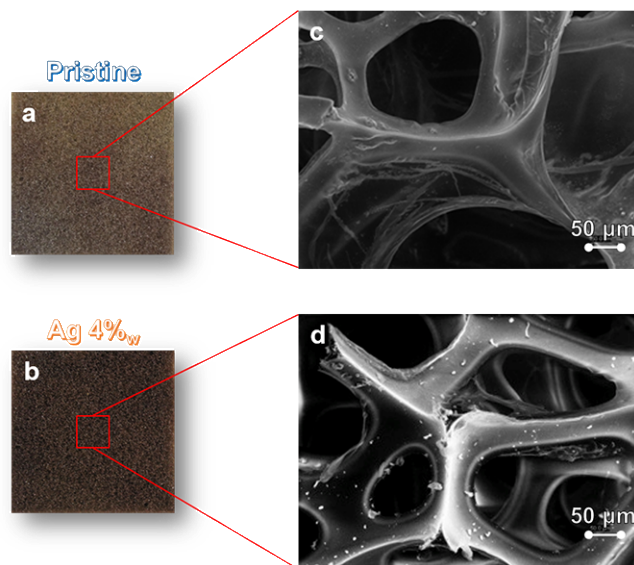


Figure 1. Optical (a, b) and SEM (c,d) micrographs of pristine and Ag-modified PU foams.

Label (4%w) indicates the concentration of AgNO_3 precursor in the solution used for Ag photo-deposition.

Surface chemical characterization of Ag-PU foams by XPS

Both pristine and treated samples were analyzed by XPS. Surface elemental compositions are reported in **Tab. 1**, where data about 4%_{w/w} Ag-treated foams are compared to those of pristine PU. Additional data, namely, elemental compositions for other silver loadings, are reported as supporting information in **Tab. S2**.

Table 1. Surface elemental composition estimated by X-ray photoelectron spectroscopy (XPS) of samples treated with 4%_{w/w} AgNPs. Error is expressed as the larger value between the error associated to a single quantification (0.2% for silver, 0.5% for other elements) and one standard deviation, calculated on at least three replicate analyses. Data about pristine samples are reported for comparison.

Sample	Pristine	Ag 4% _{w/w}
Element	At%	At%
C	69.4 ± 0.5	68.0 ± 3.0
O	22.0 ± 0.5	20.0 ± 1.0
N	3.1 ± 0.5	4.8 ± 0.8
Si	5.5 ± 0.5	2.4 ± 0.5

Ag	/	4.8 ± 0.3
----	---	---------------

Carbon and oxygen were the most abundant elements on the analyzed surfaces, as expected for an oxygenated polymer matrix modified by low amounts of inorganic NPs. Silicon traces were also detected, as common contaminants in industrial PUs^{36,37}. Obviously, no silver was detected on pristine PU samples. Ag surface atomic % was found to be a function of nominal AgNO₃ loading into the deposition bath, on treated samples (as shown by data in **Tab. 1** and in **Tab. S2**), demonstrating how the patented protocol here applied to PUs is effective in tuning the amount of inorganic NPs into the final products. XP high-resolution (HR) regions (**Fig. 2**) were also investigated, in order to obtain detailed information about surface chemical speciation in PU and AgNP phases. HR XP C1s spectra of pristine (**Fig. 2a**) and treated (**Fig. 2b**) PU foams both showed three components. Even after Ag treatment, C1s signal components remained almost unchanged. The three carbon chemical environments could be easily attributed to typical functionalities of polyurethanes^{38,39}. Only the aliphatic component at low binding energy (BE) appeared affected by an additional contribution due to adventitious hydrocarbon contamination, being more intense than what expected for a PU matrix. HR N1s regions (**Fig. 2c-d**) were acquired to assess whether the silver nitrate salt -used as AgNP precursor in photo-deposition baths- remained unreacted (or not completely removed) on sample surfaces. As reported in the Experimental section, in fact, photo-deposition baths use silver nitrate (AgNO₃) to produce Ag clusters. N1s position associated to nitrate (NO₃⁻) anion fell at 407 ± 1 eV³⁹, which is a position easily distinguishable from the one typically attributable to nitrogen of polyurethane nature, at 400 ± 1 eV^{38,39}. It is worth noting that the intensity of N1s component related to nitrate showed a dependence on the nominal Ag loading into the precursor solution. As shown in **Fig. S2a**, in fact, for a 2%_{w/w} loading, it was less intense in respect to what observed in 4%_{w/w}-related spectrum. Results obtained from the study of N1s

regions were confirmed by further investigation of the characteristic silver HR regions, i.e. Ag3d_{5/2} (main component of the Ag3d photoelectric signal) and AgM₄₅N₄₅N₄₅ (Auger signal).

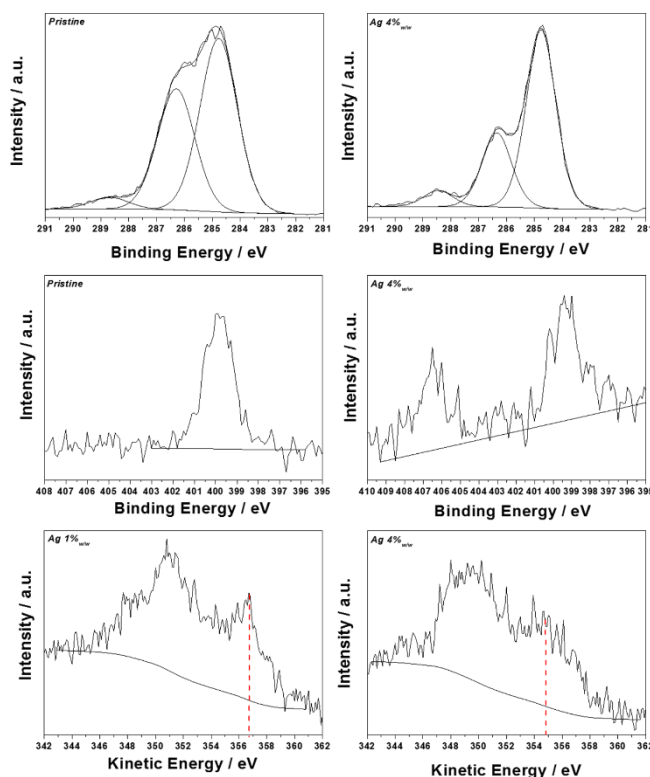


Figure 2. Typical XP HR spectra of pristine and Ag-treated samples. C1s XP-HR of pristine (a) and 4%_{w/w}-treated (b) PU; N1s XP-HR of pristine (c) and 4%_{w/w}-treated (d) PU; AgM₄₅N₄₅N₄₅ XP-HR of 1%_{w/w}-treated (e) and 4%_{w/w}-treated (f) PU.

The detailed analysis of these regions allows for determining silver chemical environments^{40,41} on treated PU surface. In particular, the discrimination between Ag⁰, Ag₂O and AgNO₃ is possible based on the kinetic energy (KE) associated to AgMNN signals. Moreover, the sum of BE of Ag3d_{5/2} and KE of AgMNN gives the modified Auger parameter (α'), useful for addressing Ag chemical speciation^{32,41}. A typical Ag3d_{5/2} spectrum is reported in **Fig. S2b**; the signal was centered at 368.5 ± 0.2 eV, at all precursor concentrations. Actually, this was not surprising, because of the very small spectral differences between different silver chemical states⁴². Anyhow, the signal related to AgMNN is much more informative, as its position changed from 356.7 ± 0.2 eV for samples treated with 1%_{w/w} AgNO₃ concentration in the photo-deposition medium (**Fig.**

2e), to 354.8 ± 0.2 eV for foams modified with a 4%_{w/w} precursor loading (**Fig. 2f**). In the first case, the value was compatible with the presence of partially oxidized Ag⁰ nanoclusters (intermediate state between Ag⁰ and Ag₂O)³⁹. The value found for foams treated with 4%_{w/w} AgNO₃ was on the contrary mainly attributable to the surface predominance of unreacted silver nitrate³⁹. Evidences on calculated Ag α' values and on the lineshape of N1s HRRs³⁹ were consistent with this interpretation.

Cross-section SEM morphological characterization of Ag-treated foams

Cross-section SEM measurements were used to assess Ag clusters distribution within treated PU foams. **Fig. 3** depicts images obtained at different depths. The images here presented clearly show that Ag nanophases distribution into PUs is particularly homogeneous. The presence of metal clusters could be appreciated up to 5 mm from the surface; this could be explained considering the easy penetration of the solution containing the metal precursor within foam pores during the modification process. High-magnification micrographs (lower panels, **Fig. 3**) allowed for evaluating AgNP particle size.

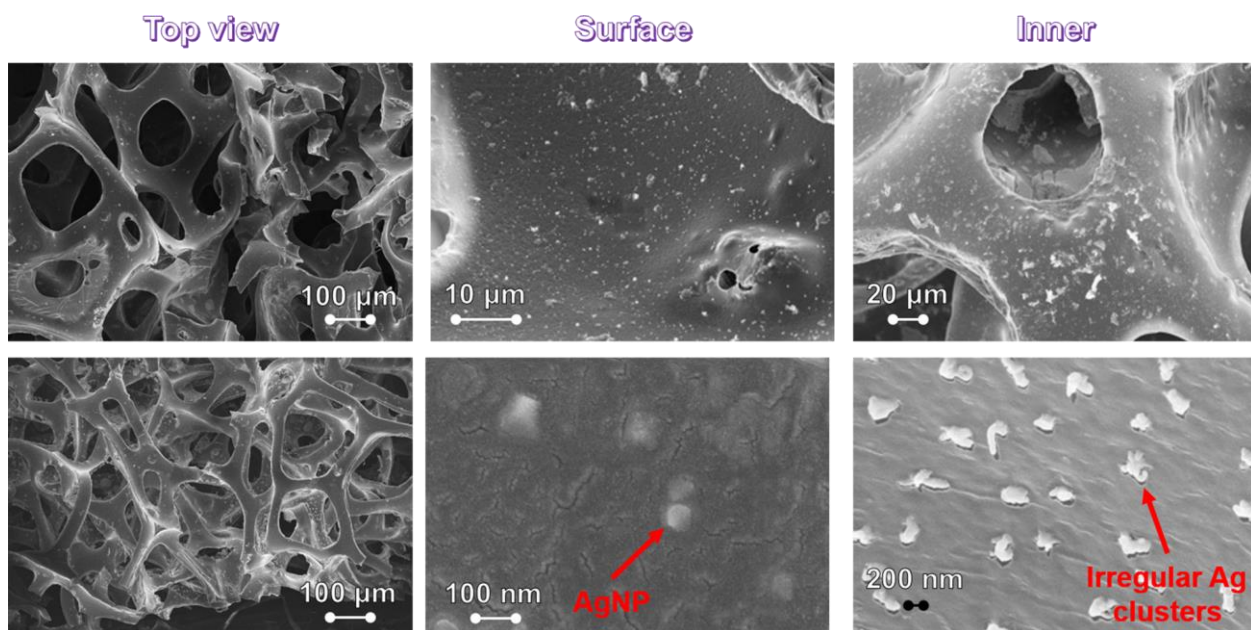


Figure 3. Cross-sectional SEM micrographs of 4%_{w/w}-treated foams.

Cluster size did not change significantly with depth: average size was 150 ± 50 nm for surface NPs, and 200 ± 50 nm for inner ones. The main difference between surface and inner layers resided in the different morphology of Ag nanophases: spheroidal particles were substituted by irregularly-shaped clusters going from surface to inner portions of the treated foam. This may be reasonably interpreted considering a less effective precursor photo-reduction at PU inner layers, where the incident radiation is attenuated by the polymer itself. Hence, irregular clusters could be attributed to the presence of partially reacted silver salt; these findings are in agreement with XPS data, where evidence of surface AgNO₃ residuals were detectable at the highest nominal Ag loading.

Silver ionic release from PU foams by ICP-MS

The ionic release measured on treated PU filters let in contact for 24 h with 2%_{w/w} HNO₃ (protocol A) provided an indicative estimation of the maximum amount of silver ions releasable by such modified materials. It was observed that treated filters could release a maximum amount of about 20 ppm of silver ions. Such a high ion release was ascribable on the one hand, to the intrinsic morphology of these materials (high porosity, high cellulation degree), on the other hand, to the very large amount of silver clusters present on PU surface, as demonstrated by SEM characterizations. ICP-MS characterization highlighted that silver release from pristine samples, let in contact with PBS for 24 h, was typically well below 50 ppb, a negligible amount if compared with Ag⁺ concentration released by treated filters.

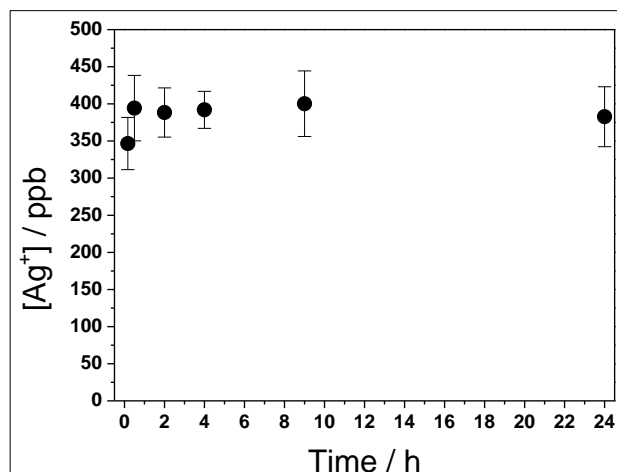


Figure 4. Silver ions release kinetics in 4%_{w/w} treated samples.

Using protocol **B**, it was possible to study the typical ionic release kinetics from Ag-treated PU left in contact with PBS solution over 24 h (see **Fig. 4**). The release was very fast and did not show any trend over time, remaining almost constant throughout the analyzed time interval, at about 400 ppb. This result was easily interpreted in terms of (i) high filters cellulation, which ensured the continuous spread of the contact medium into the inner layers of the samples, and (ii) invoking the presence of readily soluble silver species deriving from partially unreacted precursor, which was detected by XPS, and was probably responsible for the irregular shape of inorganic particles detected by SEM in the inner sections of the foam.

Nanoparticle release from PU foams: TEM analysis

The risk associated to the possible release of ultrafine AgNPs from Ag-treated PU used in air conditioning systems was assessed by TEM experiments. Liquid fractions collected after eight hours of continuous N₂ flushing through the foams, were deposited on TEM grids and systematically analyzed. Obtained micrographs did not show the presence of any structure associable to AgNPs with a diameter lower than 50 nm. In most of the analyzed TEM grids, no evidence of any particle could be detected. **Fig. 5** shows some of the very few regions of the TEM grids in which we were able to observe inorganic particles. Upper panels deal with untreated filters; lower ones are relevant to Ag-treated PUs. First of all, it was evident that the most abundant features in the micrographs were due to amorphous micron-sized structures, mostly attributable to the presence of adventitious atmospheric particulate on PU substrates. Most of all, the presence of fine (i.e. ≤ 50 nm nanostructures) on modified samples could be totally ruled out. In few cases (see for instance **Fig. 5d**), AgNPs appeared to adhere onto macroscopic PU fragments/flakes, the latter being not dangerous upon inhalation. This is indicative of an occasional release due to accidental PU fracturing, rather than to a selective AgNP detachment from the supporting foam. It is important to point out that, from a (nano-) toxicological point of view, size has been put forward as an essential parameter to predict the pulmonary inflammation caused by nanomaterials inhalation^{43–47}. It has been largely proved that smaller nanoparticles cause more pronounced adverse effects after inhalation, compared to larger (micro-) particles of the same chemical composition when applying the same mass concentrations^{44,47}. Hence, since no fine nanoparticles were released from Ag-treated PUs, the latter can be considered, in the first instance, a safe material under the toxicological point of view.

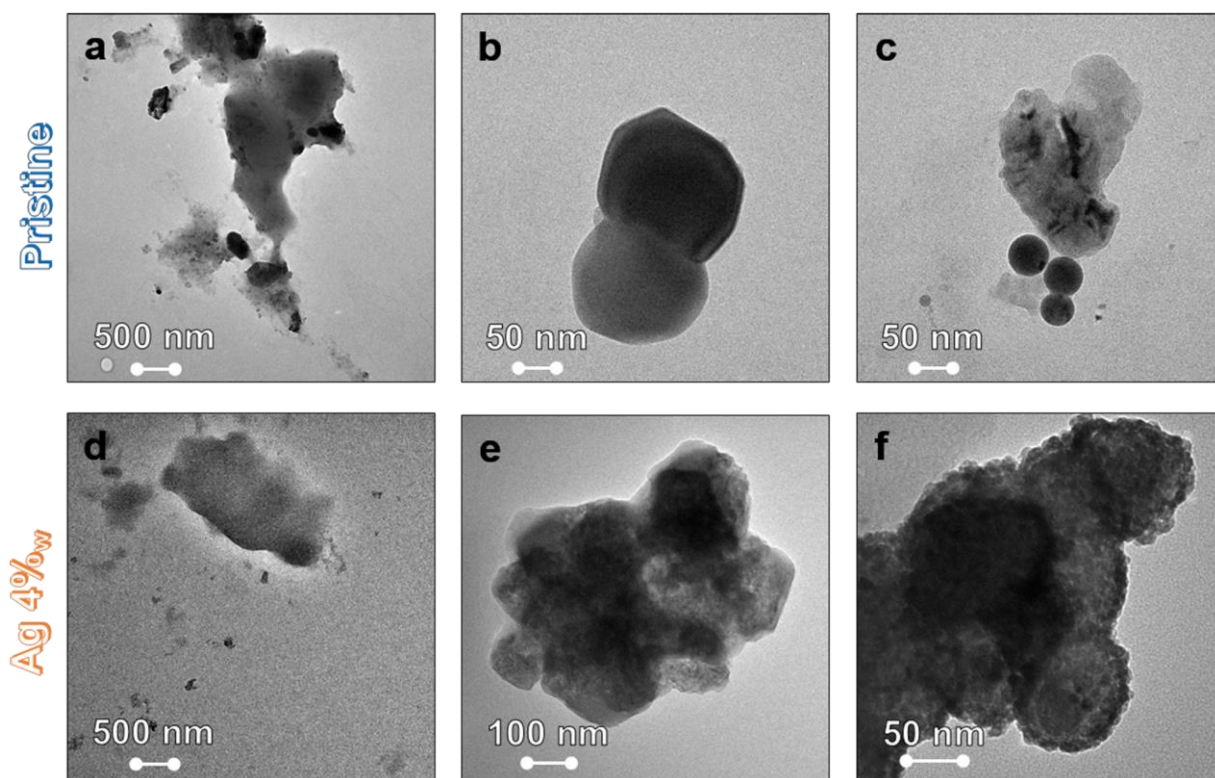


Figure 5. Nano- and micro-particle release from pristine (a-c) and Ag-treated (d-f) PU samples.

Moreover, UV-Vis experiments, done on the same samples, provided an additional evidence of such behavior, as reported in **Fig. 6**. Typical spectra acquired for pristine (black curve) and Ag-treated filters (red curve) are presented together with spectra registered on diluted solutions of AgNPs. It can be seen that the black and red curves are hardly distinguishable and present an overall absorbance of 1 mAU, while the blue curve relevant to a standard Ag nanocolloid, with a nominal silver content of ~ 10 ppb, shows a small peak, falling at ~ 435 nm in agreement with the presence of AgNPs. In the inset, a more concentrated standard Ag nanocolloid (nominal silver content of ~ 100 ppb) shows the typical and intense plasmon peak (of one order higher intensity) associated to AgNPs. The comparison with UV-Vis spectra from standard AgNPs colloids confirms the absence of quantifiable release of AgNPs from the foams of this study, either in case of samples collected from untreated PU filters (as expected) or from Ag-modified foams.

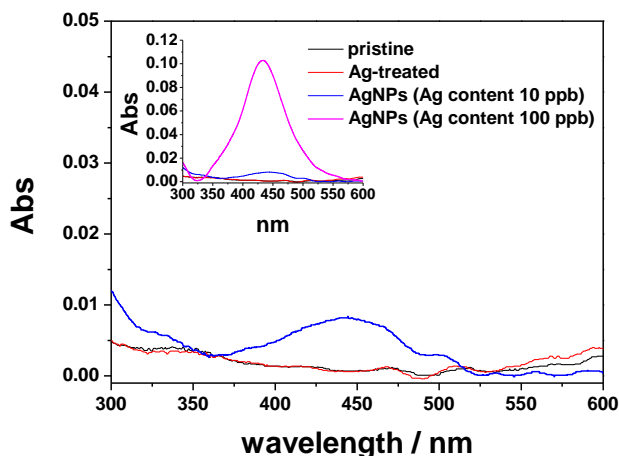


Figure 6. Typical UV-Vis spectra relevant to aqueous samples collected after release experiments with pristine (black) and Ag-treated (red) PU filters. Blue curve is relevant to UV-Vis spectrum of diluted AgNPs (Ag content ~10 ppb). In the inset, UV-Vis spectrum relevant to less diluted AgNPs (Ag content ~100 ppb) is also shown.

Antibacterial activity evaluation

The agar diffusion tests and the optical density measurements were performed on bacterial suspensions exposed to Ag-treated and untreated PU samples in order to evaluate the effect of the silver coating on two bacteria strains, namely *E. coli* and *S. aureus*, as representative Gram negative and Gram positive bacteria.

The results obtained by the agar diffusion tests are reported in **Figs. 7 and 8**. A clearly defined bacterial inhibition growth area can be observed around the silver treated samples, for both the bacterial strains (**Figs.7b-8b**).

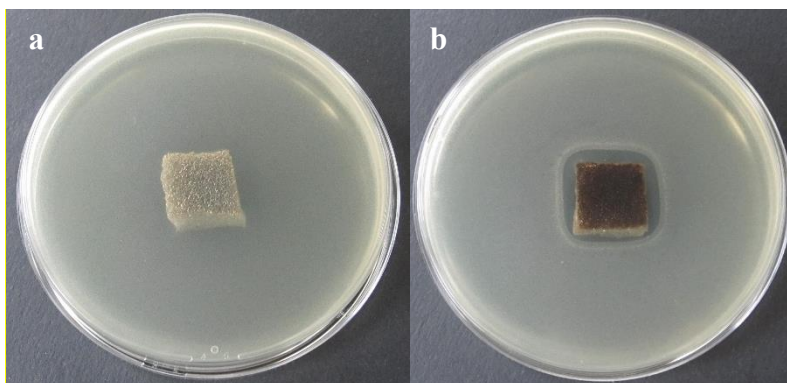


Figure 7. Agar diffusion tests on *E. coli*: (a) untreated sample, (b) silver treated sample.

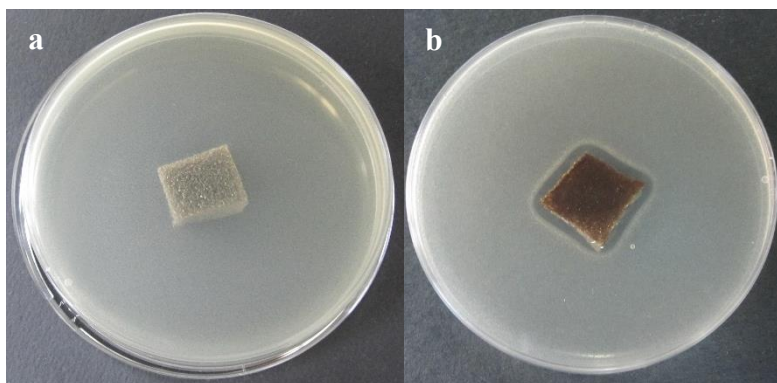


Figure 8. Agar diffusion tests on *S. aureus*: (a) untreated sample, (b) silver treated sample.

These data were confirmed by the results obtained by the bacterial enumeration reported in **Figure 9**. After incubation at 37°C, the spectrophotometric analyses demonstrated significantly reduced turbidity in the bacterial suspensions containing the silver treated PU foams, which indicated an impressive bacterial reduction associated to the AgNP-coating. Indeed, the bacterial reduction calculated after 24 hours was 97% for *E. coli* and 96% for *S. aureus* ($p < 0.01$). The bacterial suspensions were re-incubated for additional 24h to evaluate the proliferation capability of surviving bacteria (3-4%) and no bacterial growth was observed in the suspensions obtained by the silver treated samples. The values of the bacterial reduction were confirmed even after additional 24h of incubation without the samples, thus demonstrating that the low percentage of bacteria survived after 24 h are not able to proliferate and to develop resistivity to silver.

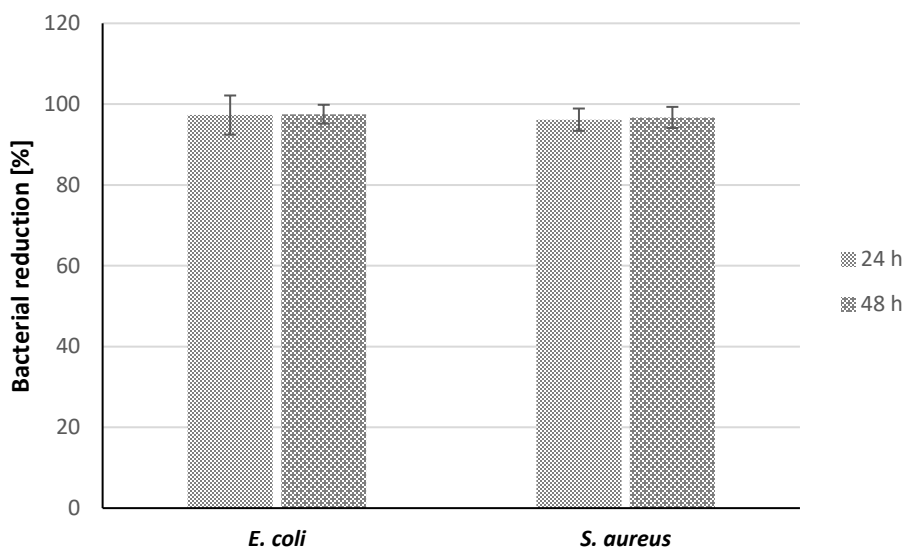


Figure 9. Bacterial reduction percentage associated to the silver treated samples in comparison with the untreated foams; bacterial re-growth calculated after 48 hours.

Cytocompatibility tests

Potential cytotoxicity associated to silver release from Ag-modified PU foams has been investigated by MTT assay on 3T3 murine fibroblasts. The results obtained, reported in **Figure 10**, were expressed as cell viability percentage compared to cells cultured without any material extract. The data demonstrated that the presence of silver does not affect the proliferative capability of 3T3 cells up to 5 days incubation, thus confirming the cytocompatibility of the silver coating deposited. Interestingly, increased cell vitality has been also observed in presence of silver ($p > 0.05$). Indeed, after 5 days incubation, the percentage of cell viability resulted 77% for the untreated samples and 84% for the silver treated samples. These results were consistent with literature data where an active role of silver in promoting cell proliferation was assessed^{32,48}.

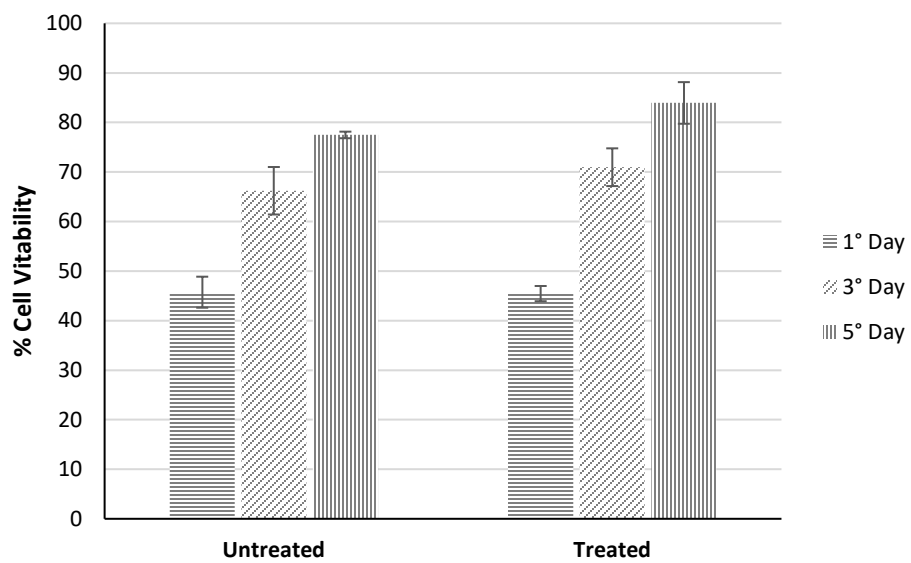


Figure 10. Cell vitality evaluated through MTT assay.

CONCLUSIONS

A photo-assisted protocol for AgNP deposition was used to modify industrial polyurethane foams. SEM and XPS analyses demonstrated that the process was effective for the tunable deposition of AgNPs onto PU filters for air filtration, without altering their porous structure and polymeric surface chemical composition. Cross-sectional SEM measurements allowed for the assessment of NP distribution within PU samples, demonstrating a good homogeneity of the in-depth distribution of Ag nanoclusters, which showed different morphologies in inner PU layers. XPS and SEM evidences suggested that partially unreacted AgNO₃ precursor could be present in inner PU layers, as well as in PUs treated with photo-deposition solutions containing the highest precursor content. ICP-MS measurements demonstrated that modified PUs were able to provide a fast release of antibacterial ions in physiological solution, which is in agreement with the presence of readily soluble Ag^(I) species on the materials surface. The absence of entire NPs release was demonstrated by mimicking a double stage filtration system; only large and amorphous clusters, ascribable to adventitious atmospheric particulate were detected, as also confirmed by UV-Vis characterization carried out on the samples. Ruling out the occurrence of ultrafine AgNP release from Ag-treated PU foams excluded *a priori* the occurrence of toxicological risks related to air-filtration application of the material herein developed. Biological tests showed that the proposed nano-functionalized materials exerted a marked inhibitory effect on the growth of different target microorganisms, without cytotoxic effects on the selected cell population.

ASSOCIATED CONTENT

Supporting Information

The following file is available free of charge (.pdf file). Operating conditions for ICP-MS analysis (Table S1), Description of the Experimental set-up for NP air release (Fig. S1), Surface elemental composition of 1%_{w/w}, 2%_{w/w} Ag-treated foams (Table S2), N1s XP region for 2%_{w/w} Ag-treated foams, and Ag3d_{5/2} XP region for 4%_{w/w} Ag-treated foams (Fig. S2).

AUTHOR INFORMATION

Corresponding Authors

[*E-mail: nicola.cioffi@uniba.it](mailto:nicola.cioffi@uniba.it), tel. +39 0805442020, [*E-mail: rosaria.picca@uniba.it](mailto:rosaria.picca@uniba.it)

Author Contributions

R.A.P. designed the characterization experiments and analyzed the data. F.P. and M.P. set up and carried out the photo-deposition process of AgNPs on PU foams; they also performed biological tests and analyzed the data. A.P. performed the cytocompatibility tests. M.C.S. contributed to the XPS characterization and wrote the first draft of the paper. L.C.G. and A.M. carried out ICP-MS measurements. C.D.F. performed SEM analysis. A.V. contributed to materials characterizations and discussion about research plan. N.C. supervised the activities and carried out TEM analysis. The manuscript was written through contributions of all authors. All authors have given approval to the final version of the manuscript.

Notes

The authors declare no competing financial interest.

ACKNOWLEDGMENTS

Lino Mondino, R & D director of Adler Group, is acknowledged for technical discussions and for kindly providing samples of polyurethane foams. Prof. Gerardo Palazzo, University of Bari, is gratefully thanked for scientific discussions and DLS and UV-Vis experiments. Financial support from MIUR (Project “Silver” PON01_02210) and from Regione Puglia (Project code 56: “Laboratorio di tecnologie di modificazione superficiale di fibre naturali per il rilancio del settore tessile in Puglia”) is gratefully acknowledged.

REFERENCES

- (1) Rezić, I. Determination of engineered nanoparticles on textiles and in textile wastewaters. *TrAC, Trends Anal. Chem.* **2011**, *30* (7), 1159–1167 DOI: 10.1016/j.trac.2011.02.017.
- (2) Benn, T.; Cavanagh, B.; Hristovski, K.; Posner, J. D.; Westerhoff, P. The Release of Nanosilver from Consumer Products Used in the Home. *Journal of Environment Quality* **2010**, *39* (6), 1875 DOI: 10.2134/jeq2009.0363.
- (3) W. Lem, K.; Choudhury, A.; A. Lakhani, A.; Kuyate, P.; R. Haw, J.; S. Lee, D.; Iqbal, Z.; J. Brumlik, C. Use of Nanosilver in Consumer Products. *Recent Patents on Nanotechnology* **2012**, *6* (1), 60–72 DOI: 10.2174/187221012798109318.
- (4) Mackevica, A.; Olsson, M. E.; Hansen, S. F. The release of silver nanoparticles from commercial toothbrushes. *Journal of Hazardous Materials* **2016**, *In press* DOI: 10.1016/j.jhazmat.2016.03.067.
- (5) Mulongo, G.; Mbabazi, J.; Nnamuyomba, P.; Hak-Chol, S. Water Bactericidal Properties of Nanosilver-Polyurethane Composites. *Nanoscience and Nanotechnology* **2012**, *1* (2), 40–42 DOI: 10.5923/j.nn.20110102.07.
- (6) Qu, R.; Gao, J.; Tang, B.; Ma, Q.; Qu, B.; Sun, C. Preparation and property of polyurethane/nanosilver complex fibers. *Applied Surface Science* **2014**, *294*, 81–88 DOI: 10.1016/j.apsusc.2013.11.116.
- (7) Chaloupka, K.; Malam, Y.; Seifalian, A. M. Nanosilver as a new generation of nanoparticle in biomedical applications. *Trends Biotechnol.* **2010**, *28* (11), 580–588 DOI: 10.1016/j.tibtech.2010.07.006.
- (8) Engels, H.-W.; Pirkel, H.-G.; Albers, R.; Albach, R. W.; Krause, J.; Hoffmann, A.; Casselmann, H.; Dormish, J. Polyurethanes: Versatile Materials and Sustainable Problem Solvers for Today's Challenges. *Angew. Chem. Int. Ed.* **2013**, *52* (36), 9422–9441 DOI: 10.1002/anie.201302766.
- (9) Zdrahala, R. J.; Zdrahala, I. J. Biomedical Applications of Polyurethanes: A Review of Past Promises, Present Realities, and a Vibrant Future. *J Biomater Appl* **1999**, *14* (1), 67–90 DOI: 10.1177/088532829901400104.
- (10) Paul, D.; Paul, S.; Roohpour, N.; Wilks, M.; Vadgama, P. Antimicrobial, Mechanical and Thermal Studies of Silver Particle-Loaded Polyurethane. *Journal of Functional Biomaterials* **2013**, *4* (4), 358–375 DOI: 10.3390/jfb4040358.
- (11) Jayakumar, R.; Lee, Y.-S.; Nanjundan, S. Studies on metal-containing copolyurethanes. *Reactive and Functional Polymers* **2003**, *55* (3), 267–276 DOI: 10.1016/S1381-5148(03)00017-8.
- (12) Liu, P.; Huang, T.; Liu, P.; Shi, S.; Chen, Q.; Li, L.; Shen, J. Zwitterionic modification of polyurethane membranes for enhancing the anti-fouling property. *Journal of Colloid and Interface Science* **2016**, *480*, 91–101 DOI: 10.1016/j.jcis.2016.07.005.
- (13) Zhang, J.; Woodruff, T. M.; Clark, R. J.; Martin, D. J.; Minchin, R. F. Release of bioactive peptides from polyurethane films in vitro and in vivo: Effect of polymer composition. *Acta Biomaterialia* **2016**, *41*, 264–272 DOI: 10.1016/j.actbio.2016.05.034.
- (14) Ciobanu, G.; Ilisei, S.; Luca, C. Hydroxyapatite-silver nanoparticles coatings on porous polyurethane scaffold. *Materials Science and Engineering: C* **2014**, *35*, 36–42 DOI: 10.1016/j.msec.2013.10.024.
- (15) Vogels, R. R. M.; Lambert, A.; Schuster, P.; Jockenhoevel, S.; Bouvy, N. D.; Disselhorst-Klug, C.; Neumann, U. P.; Klinge, U.; Klink, C. D. Biocompatibility and biomechanical

- analysis of elastic TPU threads as new suture material. *J. Biomed. Mater. Res.* **2015**, n/a-n/a DOI: 10.1002/jbm.b.33531.
- (16) Sin, D.; Miao, X.; Liu, G.; Wei, F.; Chadwick, G.; Yan, C.; Friis, T. Polyurethane (PU) scaffolds prepared by solvent casting/particulate leaching (SCPL) combined with centrifugation. *Materials Science and Engineering: C* **2010**, 30 (1), 78–85 DOI: 10.1016/j.msec.2009.09.002.
 - (17) Burke, A.; Hasirci, N. Polyurethanes in Biomedical Applications. In *Biomaterials*; Hasirci, N., Hasirci, V., Eds.; Advances in Experimental Medicine and Biology; Springer US, 2004; pp 83–101.
 - (18) Grasl, C.; Bergmeister, H.; Stoiber, M.; Schima, H.; Weigel, G. Electrospun polyurethane vascular grafts: In vitro mechanical behavior and endothelial adhesion molecule expression. *J. Biomed. Mater. Res.* **2010**, 93A (2), 716–723 DOI: 10.1002/jbm.a.32584.
 - (19) Maya, I. D.; Weatherspoon, J.; Young, C. J.; Barker, J.; Allon, M. Increased Risk of Infection Associated with Polyurethane Dialysis Grafts. *Seminars in Dialysis* **2007**, 20 (6), 616–620 DOI: 10.1111/j.1525-139X.2007.00372.x.
 - (20) Francolini, I.; Ruggeri, V.; Martinelli, A.; D’Ilario, L.; Piozzi, A. Novel Metal-Polyurethane Complexes with Enhanced Antimicrobial Activity. *Macromol. Rapid Commun.* **2006**, 27 (4), 233–237 DOI: 10.1002/marc.200500786.
 - (21) Roohpour, N.; Moshaverinia, A.; Wasikiewicz, J. M.; Paul, D.; Wilks, M.; Michael Millar; Vadgama, P. Development of bacterially resistant polyurethane for coating medical devices. *Biomed. Mater.* **2012**, 7 (1), 015007 DOI: 10.1088/1748-6041/7/1/015007.
 - (22) Sportelli, M. C.; Picca, R. A.; Cioffi, N. Recent advances in the synthesis and characterization of nano-antimicrobials. *TrAC, Trends Anal. Chem.* **2016** DOI: 10.1016/j.trac.2016.05.002.
 - (23) The Nanodatabase <http://nanodb.dk/>.
 - (24) Franci, G.; Falanga, A.; Galdiero, S.; Palomba, L.; Rai, M.; Morelli, G.; Galdiero, M. Silver Nanoparticles as Potential Antibacterial Agents. *Molecules* **2015**, 20 (5), 8856–8874 DOI: 10.3390/molecules20058856.
 - (25) Prabhu, S.; Poulse, E. K. Silver nanoparticles: mechanism of antimicrobial action, synthesis, medical applications, and toxicity effects. *Int Nano Lett* **2012**, 2 (1), 32 DOI: 10.1186/2228-5326-2-32.
 - (26) Taheri, S.; Cavallaro, A.; Christo, S. N.; Majewski, P.; Barton, M.; Hayball, J. D.; Vasilev, K. Antibacterial Plasma Polymer Films Conjugated with Phospholipid Encapsulated Silver Nanoparticles. *ACS Biomater. Sci. Eng.* **2015**, 1 (12), 1278–1286 DOI: 10.1021/acsbiomaterials.5b00338.
 - (27) Durán, N.; Durán, M.; de Jesus, M. B.; Seabra, A. B.; Fávaro, W. J.; Nakazato, G. Silver nanoparticles: A new view on mechanistic aspects on antimicrobial activity. *Nanomedicine: Nanotech. Biol. Med.* **2016**, 12 (3), 789–799 DOI: 10.1016/j.nano.2015.11.016.
 - (28) Paladini, F.; Cooper, I. R.; Pollini, M. Development of antibacterial and antifungal silver-coated polyurethane foams as air filtration units for the prevention of respiratory diseases. *J Appl Microbiol* **2014**, 116 (3), 710–717 DOI: 10.1111/jam.12402.
 - (29) Sharma, V. K.; Yngard, R. A.; Lin, Y. Silver nanoparticles: Green synthesis and their antimicrobial activities. *Advances in Colloid and Interface Science* **2009**, 145 (1–2), 83–96 DOI: 10.1016/j.cis.2008.09.002.

- (30) Vukomanović, M.; Repnik, U.; Zavašnik-Bergant, T.; Kostanjšek, R.; Škapin, S. D.; Suvorov, D. Is Nano-Silver Safe within Bioactive Hydroxyapatite Composites? *ACS Biomater. Sci. Eng.* **2015**, *1* (10), 935–946 DOI: 10.1021/acsbiomaterials.5b00170.
- (31) Pollini, M.; Sannino, A.; Maffezzoli, A.; Licciulli, A. Antibacterial surface treatments based on silver clusters deposition. WO/2007/074484, 2007.
- (32) Paladini, F.; Picca, R. A.; Sportelli, M. C.; Cioffi, N.; Sannino, A.; Pollini, M. Surface chemical and biological characterization of flax fabrics modified with silver nanoparticles for biomedical applications. *Materials Science and Engineering C* **2015**, *52*, 1–10 DOI: 10.1016/j.msec.2015.03.035.
- (33) Quadros, M. E.; Marr, L. C. Environmental and Human Health Risks of Aerosolized Silver Nanoparticles. *Journal of the Air & Waste Management Association* **2010**, *60* (7), 770–781 DOI: 10.3155/1047-3289.60.7.770.
- (34) Althouse, A. D.; Turnquist, C. H.; Bracciano, A. F.; Bracciano, D. C.; Bracciano, G. M. *Modern Refrigeration and Air Conditioning, 19th Edition*, 19th ed.; Goodheart-Willcox Publisher, 2014.
- (35) Panáček, A.; Kvítek, L.; Prucek, R.; Kolář, M.; Večeřová, R.; Pizúrová, N.; Sharma, V. K.; Nevěčná, T.; Zbořil, R. Silver Colloid Nanoparticles: Synthesis, Characterization, and Their Antibacterial Activity. *J. Phys. Chem. B* **2006**, *110* (33), 16248–16253 DOI: 10.1021/jp063826h.
- (36) Ditaranto, N.; Picca, R. A.; Sportelli, M. C.; Sabbatini, L.; Cioffi, N. Surface characterization of manufactured goods modified by metal/metal oxides nano-antimicrobials. *Surface and Interface Analysis* **2016**, *48*, 505–508 DOI: 10.1002/sia.5951.
- (37) Sportelli, M. C.; Picca, R. A.; Ronco, R.; Bonerba, E.; Tantillo, G.; Pollini, M.; Sannino, A.; Valentini, A.; Cataldi, T. R. I.; Cioffi, N. Investigation of Industrial Polyurethane Foams Modified with Antimicrobial Copper Nanoparticles. *Materials* **2016**, *9* (7), 544 DOI: 10.3390/ma9070544.
- (38) Hearn, M. J.; Ratner, B. D.; Briggs, D. SIMS and XPS studies of polyurethane surfaces. 1. Preliminary studies. *Macromolecules* **1988**, *21* (10), 2950–2959 DOI: 10.1021/ma00188a011.
- (39) NIST XPS Database <http://srdata.nist.gov/xps>.
- (40) Bera, S.; Gangopadhyay, P.; Nair, K. G. M.; Panigrahi, B. K.; Narasimhan, S. V. Electron spectroscopic analysis of silver nanoparticles in a soda-glass matrix. *Journal of Electron Spectroscopy and Related Phenomena* **2006**, *152* (1–2), 91–95 DOI: 10.1016/j.elspec.2006.03.008.
- (41) Cioffi, N.; Colaianni, L.; Pilolli, R.; Calvano, C.; Palmisano, F.; Zambonin, P. Silver nanofractals: electrochemical synthesis, XPS characterization and application in LDI-MS. *Anal. Bioanal. Chem.* **2009**, *394* (5), 1375–1383 DOI: 10.1007/s00216-009-2820-y.
- (42) Wagner, C. D.; Gale, L. H.; Raymond, R. H. Two-dimensional chemical state plots: a standardized data set for use in identifying chemical states by x-ray photoelectron spectroscopy. *Anal. Chem.* **1979**, *51* (4), 466–482 DOI: 10.1021/ac50040a005.
- (43) Braakhuis, H. M.; Cassee, F. R.; Fokkens, P. H. B.; Fonteyne, L. J. J. de la; Oomen, A. G.; Krystek, P.; Jong, W. H. de; Loveren, H. van; Park, M. V. D. Z. Identification of the appropriate dose metric for pulmonary inflammation of silver nanoparticles in an inhalation toxicity study. *Nanotoxicology* **2016**, *10* (1), 63–73 DOI: 10.3109/17435390.2015.1012184.

- (44) Kim, I.-Y.; Joachim, E.; Choi, H.; Kim, K. Toxicity of silica nanoparticles depends on size, dose, and cell type. *Nanomedicine* **2015**, *11* (6), 1407–1416 DOI: 10.1016/j.nano.2015.03.004.
- (45) Sung, J. H.; Ji, J. H.; Park, J. D.; Yoon, J. U.; Kim, D. S.; Jeon, K. S.; Song, M. Y.; Jeong, J.; Han, B. S.; Han, J. H.; et al. Subchronic Inhalation Toxicity of Silver Nanoparticles. *Toxicol. Sci.* **2009**, *108* (2), 452–461 DOI: 10.1093/toxsci/kfn246.
- (46) Braakhuis, H. M.; Gosens, I.; Krystek, P.; Boere, J. A.; Cassee, F. R.; Fokkens, P. H.; Post, J. A.; van Loveren, H.; Park, M. V. Particle size dependent deposition and pulmonary inflammation after short-term inhalation of silver nanoparticles. *Part and Fibre Toxicol* **2014**, *11*, 49 DOI: 10.1186/s12989-014-0049-1.
- (47) Patchin, E. S.; Anderson, D. S.; Silva, R. M.; Uyeminami, D. L.; Scott, G. M.; Guo, T.; Van Winkle, L. S.; Pinkerton, K. E. Size-Dependent Deposition, Translocation, and Microglial Activation of Inhaled Silver Nanoparticles in the Rodent Nose and Brain. *Environ Health Perspect* **2016** DOI: 10.1289/EHP234.
- (48) Liu, X.; Lee, P.; Ho, C.; Lui, V. C. H.; Chen, Y.; Che, C.; Tam, P. K. H.; Wong, K. K. Y. Silver Nanoparticles Mediate Differential Responses in Keratinocytes and Fibroblasts during Skin Wound Healing. *ChemMedChem* **2010**, *5* (3), 468–475 DOI: 10.1002/cmdc.200900502.

Graphic - For Table of Contents Only

